Progressive maturation of silent synapses governs the duration of a critical period

Xiaojie Huang[a,b,1], Sophia K. Stodieck[b,c,1], Bianka Goetze[c], Lei Cui[a,b], Man Ho Wong[a,b], Colin Wenzel[c], Leon Hosang[c], Yan Dong[d], Siegrid Löwel[c,e,2,3], and Oliver M. Schlüter[a,e,2,3]

[a]Molecular Neurobiology, European Neuroscience Institute, D-37077 Göttingen, Germany; [b]Göttingen Graduate School for Neurosciences and Molecular Biosciences, D-37077 Göttingen, Germany; [c]Bernstein Fokus Neurotechnologie and Department of Systems Neuroscience, Johann-Friedrich-Blumenbach Institut für Zoologie und Anthropologie, Universität Göttingen, D-37075 Göttingen, Germany; [d]Department of Neuroscience, University of Pittsburgh, Pittsburgh, PA 15260; and [e]Sensory Collaborative Research Center 889, University of Göttingen, D-37075 Göttingen, Germany

Edited by Thomas C. Südhof, Stanford University School of Medicine, Stanford, CA, and approved May 1, 2015 (received for review April 1, 2015)

During critical periods, all cortical neural circuits are refined to optimize their functional properties. The prevailing notion is that the balance between excitation and inhibition determines the onset and closure of critical periods. In contrast, we show that maturation of silent glutamatergic synapses onto principal neurons was sufficient to govern the duration of the critical period for ocular dominance plasticity in the visual cortex of mice. Specifically, postsynaptic density protein-95 (PSD-95) was absolutely required for experience-dependent maturation of silent synapses, and its absence before the onset of critical periods resulted in lifelong juvenile ocular dominance plasticity. Loss of PSD-95 in the visual cortex after the closure of the critical period reinstated silent synapses, resulting in reopening of juvenile-like ocular dominance plasticity. Additionally, silent synapse-based ocular dominance plasticity was largely independent of the inhibitory tone, whose developmental maturation was independent of PSD-95. Moreover, glutamatergic synaptic transmission onto parvalbumin-positive interneurons was unaltered in PSD-95 KO mice. These findings reveal not only that PSD-95–dependent silent synapse maturation in visual cortical principal neurons terminates the critical period for ocular dominance plasticity but also indicate that, in general, once silent synapses are consolidated in any neural circuit, initial experience-dependent functional optimization and critical periods end.

critical period | ocular dominance plasticity | silent synapse | PSD-95 | visual cortex

Immature cortical neural networks, which are formed primarily under genetic control (1), require experience and training to shape and optimize their functional properties. This experience-dependent refinement is considered to be a general developmental process for all functional cortical domains and typically peaks during their respective critical periods (CPs) (2, 3). Known examples for CPs span functional domains as diverse as filial imprinting and courtship song learning in birds (4, 5); cognitive functions, such as linguistic or musical skills in humans (6, 7); and likely best studied, the different features of sensory modalities (3). CPs are characterized by the absolute requirement for experience in a restricted time window for neural network optimization. Lack of visual experience during the CP for visual cortex refinements can, for example, cause irreversible visual impairment (8). Refinements during the CP play an essential role (9). Although some functions can be substantially ameliorated after the CP, they are rarely optimally restored.

It is believed that the neural network refinement is based on synapse stabilization and elimination (10–12) and includes forms of long-term synaptic plasticity to remodel excitatory synapses of principal neurons (13, 14). Although long-term plasticity at these excitatory synapses is instructive for shaping neural networks for functional output and their expression coincides with CPs, it is not known whether the remodeling itself governs the duration of CPs. In contrast, only permissive mechanisms have been shown to terminate CPs. Among these, the developmental increase of local inhibition appears to be the dominating mechanism to regulate cortical plasticity and CPs (15–17). Additionally, extracellular matrix remodeling is involved, as well as receptors of immune signaling, such as paired Ig-like receptor B (PirB), or axon pathfinding, such as Nogo (18–21). However, a specific function to directly regulate synapse remodeling during initial neural network optimization is not known and a potential instructive function of PirB was described for adult cortical plasticity but not plasticity of the initial synapse remodeling during CPs (22).

AMPA receptor-silent synapses have been proposed to be efficient plasticity substrates during early cortical network refinements (13, 23, 24). Silent synapses are thought to be immature, still-developing excitatory synapses containing only NMDA receptors (NMDARs) but lacking AMPA receptors (AMPARs) (23, 24). They are functionally dormant but can evolve into fully transmitting synapses by experience-dependent insertion of AMPARs, a plasticity process thought to occur frequently in developing cortices (10). Although they appear as the ideal synaptic substrate for CP plasticity and their maturation correlates with sensory experience (10, 25), it has not been experimentally tested whether maturation of silent synapses indeed causes the termination of critical periods. This conceptual model contrasts with the current view that increased local inhibition and the expression of plasticity brakes ends critical periods (18–20, 26).

Significance

During critical periods, cortical neural circuits are refined to optimize their functional properties. The prevailing notion is that the balance between excitation and inhibition determines the onset and closure of critical periods. Here, we show that postsynaptic density protein-95 (PSD-95)–dependent maturation of silent glutamatergic synapses onto principal neurons was sufficient to govern the duration of the critical period for ocular dominance plasticity (ODP) in the visual cortex of mice. Loss of PSD-95 before the onset of CPs resulted in lifelong ODP, loss after CP closure reinstated silent synapses, and ODP. Thus, PSD-95–dependent silent synapse maturation terminates the critical period of ODP, and in general, once silent synapses are consolidated in any neural circuit, critical periods may end.

Author contributions: X.H., S.K.S., B.G., Y.D., S.L., and O.M.S. designed research; X.H., S.K.S., B.G., L.C., M.H.W., C.W., L.H., and O.M.S. performed research; X.H., S.K.S., B.G., L.C., M.H.W., C.W., L.H., S.L., and O.M.S. analyzed data; and Y.D., S.L., and O.M.S. wrote the paper.

The authors declare no conflict of interest.

This article is a PNAS Direct Submission.

Freely available online through the PNAS open access option.

[1]X.H. and S.K.S. contributed equally to this work.

[2]S.L. and O.M.S. contributed equally to this work.

[3]To whom correspondence may be addressed. Email: sloewel@gwdg.de or oschlue@gwdg.de.

This article contains supporting information online at www.pnas.org/lookup/suppl/doi:10.1073/pnas.1506488112/-/DCSupplemental.

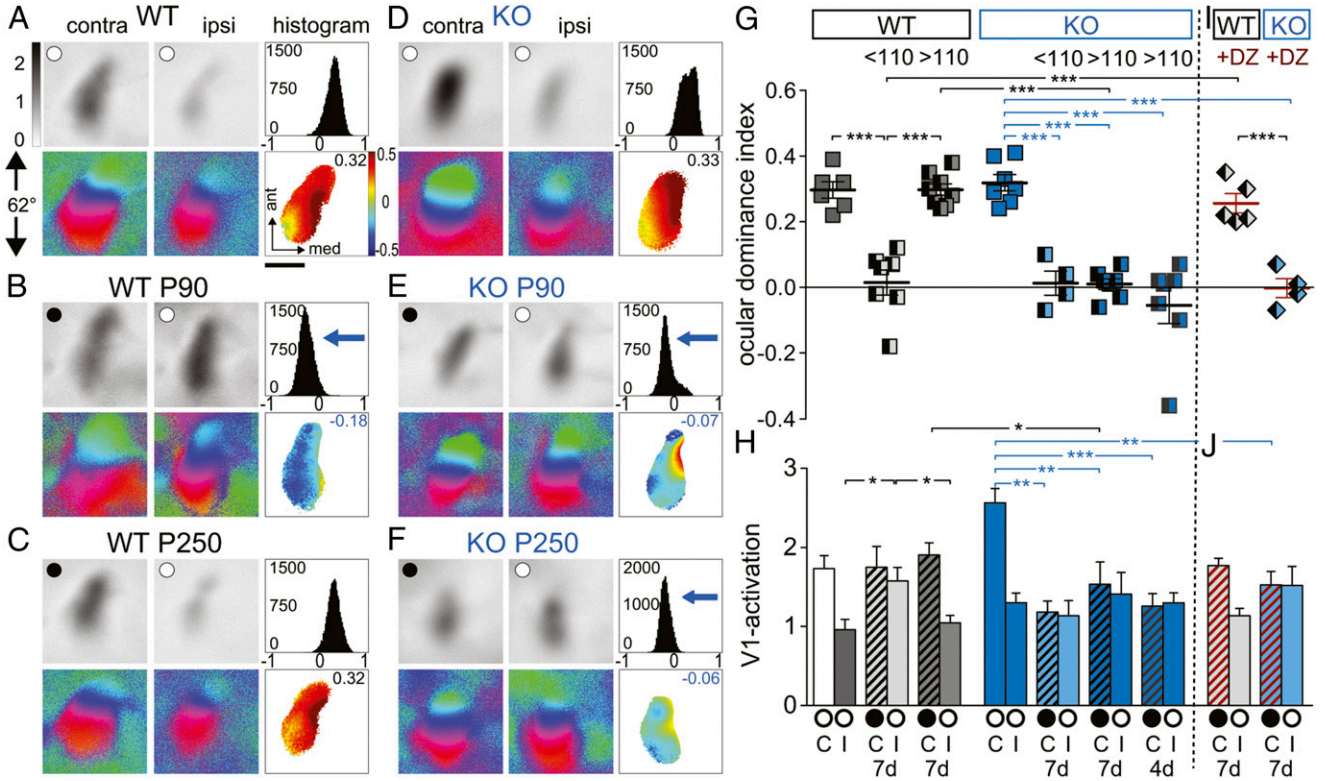

Fig. 1. PSD-95 KO mice displayed juvenile-like ocular dominance plasticity into late adulthood. Optically imaged activity maps in V1 of WT (*A–C*) and PSD-95 KO mice (*D–F*) of 3- (P90) and 8-mo-old (P250) mice before (*A* and *D*) and after 7 d of MD (*B*, *C*, *E*, and *F*), and their quantification (*G* and *H*). ○, open eyes; ●, deprived eyes. (*A–F*) Grayscale coded response magnitude maps (top rows, expressed as fractional change in reflectance $\times 10^{-4}$), color-coded maps of retinotopy (bottom rows), histogram of OD scores (top right of panels), and color-coded OD map [bottom right including average OD index (ODI) value] are illustrated. In control mice of both genotypes (*A* and *D*), activity patches evoked by stimulation of the contralateral (contra) eye were always darker than those evoked by ipsilateral eye (ipsi) stimulation, the average ODI was positive, and warm colors prevailed in the 2D OD map indicating contralateral dominance. After 7 d of MD, there was an OD shift toward the open eye in PSD-95 KO mice of all tested ages (*E* and *F*): the ODI histogram shifted leftward, the ODI decreased, and colder colors prevailed in the OD map (negative ODI values). In contrast, in WT mice, ODP was absent beyond P110 (compare *B* and *C*). (Scale bar, 1 mm.) ODIs (*G*) and V1 activation (*H*) before (oo) and after (●o) MD (7 or 4 d) in PSD-95 KO and WT mice below (<P110) and above P110 (>P110). Symbols in *G* represent ODI values of individuals; means are marked by horizontal lines. (*H*) V1 activation elicited by stimulation of the contralateral (C) or ipsilateral (I) eye. (*I* and *J*) OD indices (*I*) and V1 activation (*J*) after (●o) monocular deprivation (7 d) in PSD-95 KO and WT mice after diazepam-treatment (+DZ): juvenile ODP persisted in PSD-95 KO but not in WT mice after DZ treatment. Layout as in *G* and *H*. $*P < 0.05$; $**P < 0.01$; $***P < 0.001$. Values in Table S1.

We hypothesize that experience-dependent unsilencing of silent synapses, which results in strengthening and maturation of excitatory synapses, governs network stabilization and refinement during critical periods, and that the progressive decrease of silent synapses leads to the closure of critical periods.

Experience-dependent cortical plasticity is classically tested with ocular dominance (OD) plasticity (ODP) in the primary visual cortex (V1), induced by monocular deprivation (MD). In the binocular region of mouse V1, neurons respond to sensory inputs from both eyes, but activity is dominated by afferents from the contralateral eye. During the critical period, a brief MD induces an OD shift of visually evoked responses in V1 toward the open eye (27–29). This juvenile ODP is mediated by a reduction of deprived eye responses in V1 and is temporally confined to a critical period (30, 31).

A molecular candidate regulating the cellular basis of critical period plasticity is postsynaptic density protein-95 (PSD-95), whose expression in the visual cortex increases on eye opening and thus the onset of visual experience (32). PSD-95 promotes the maturation of AMPA receptor-silent excitatory synapses in hippocampal neurons and is required for activity-driven synapse stabilization (33–35). In juvenile PSD-95 KO mice, ODP displays the same features as in WT mice (36). However, as adult PSD-95 KO mice have not yet been analyzed, it is unknown whether PSD-95 is essential for the closure of critical periods. Thus, PSD-95 appeared to be the ideal molecular candidate to test our conceptual model that progressive silent synapse maturation marks the closure of critical periods.

Results

The Juvenile Form of Ocular Dominance Plasticity Is Preserved in PSD-95 KO Until Late Adulthood. Given the role of PSD-95 in synapse maturation, we tested here whether loss of PSD-95 affects the closure of the critical period for juvenile ODP. In adult PSD-95 KO mice, similar to WT mice, V1 was dominated by visual input from the contralateral eye (Fig. 1 *A, D, G*, and *H*). However, in contrast to standard cage raised WT mice, which lack ODP beyond P110 (37), a 7-d MD in PSD-95 KO mice induced an OD shift toward the open eye at an age up to 1.5 y (P507) (Fig. 1 *C* and *G*). This OD shift in old (>P110) PSD-95 KO mice was mediated by a reduction of deprived eye responses in V1 (Fig. 1 *E, F*, and *H*), which is characteristic for ODP during the critical period (30). Another hallmark of juvenile-like ODP is that relatively short MD triggers it (31). This hallmark was present in PSD-95 KO mice at least up to P480, in which a 4-d MD was sufficient to induce juvenile-like ODP (Fig. 1 *G* and *H*). In contrast, in WT mice <P110, a 7-d MD was needed to induce an OD shift. This shift was primarily mediated by an increase of open eye responses in V1 (Fig. 1 *B* and *H*), whereas the decrease in deprived eye responses was absent (Fig. 1 *B* and *H*). This

result is typical for adult, noncritical period-like ODP (30). Thus, characteristic features of juvenile ODP were present in V1 of adult KO mice but not in adult WT mice (38). These findings indicate that critical period plasticity in V1 is maintained lifelong in V1 of PSD-95 KO mice, and the cellular mechanisms underlying ODP retain its juvenile form.

The Basic Organization of Visual Cortex and Basic Visual Performance Are Largely Normal in PSD-95 KO Mice. To test whether basic visual performance is compromised in the PSD-95 KO mice, we analyzed V1 topographic maps quantitatively, activated by either horizontally or vertically moving bars presented to the contralateral eye (Fig. S1 *A* and *D*). Retinotopic map quality was similar in PSD-95 KO and WT mice, indicating a normal topographic activation (Fig. S1). The signal intensity of V1 activation was higher in PSD-95 KO mice for elevation but not azimuth stimuli (Fig. S1 *H* and *J*). We then tested visual acuity with the visual water task (VWT), a visual discrimination task based on reinforcement learning (39). In this test, mice were trained to distinguish a vertical sine wave grating displayed on one monitor from isoluminent gray on another monitor in a trapezoid pool with shallow water (Fig. S1*K*). The grating was randomly presented on either monitor and paired with an invisible escape platform below the water surface to enforce swimming toward it. After the mice had learned the task, the spatial frequency of the grating was gradually increased to test their visual acuity limit. PSD-95 KO mice had similar average visual acuity of ∼0.5 cycles/deg as WT mice (Fig. S1*L*). This result demonstrates that PSD-95 KO mice are able to learn an associative visual task and that their visual acuity is not compromised.

Silent Synapse Maturation Is Impaired in V1 of PSD-95 KO Mice. At the beginning of postnatal brain development, AMPA receptor-silent excitatory synapses are abundant (13, 23, 24, 40). Because the number of silent synapses is elevated in the hippocampus of PSD-95 KO mice (35), we tested whether the conversion of silent to mature synapses was also impaired in the visual cortex and whether PSD-95–based conversion is required for the termination of the CP for ODP. We compared the number of silent synapses between PSD-95 KO and WT mice before eye opening (P10–12), during (P25–30), and after the CP for ODP (P60–70) (3). We used the minimal stimulation assay to assess the level of silent synapses (24) (Fig. 2 *B* and *C*) of excitatory projections from layer 4 (L4) to L2/3 pyramidal cells in V1 (Fig. 2*A*), where developmental refinements occur for OD during the CP (41). In WT mice, the fraction of silent synapses among total synapses was ∼55% on P10–12, dropped to ∼25% on P25–30, and dropped further down to ∼5% on P60–70 (Fig. 2*D*), indicating that ∼50% of total number of synapses was silent at eye opening and this fraction progressively declined in an experience-dependent maturation process. In PSD-95 KO mice, the fraction of silent synapses was similar to WT mice before eye opening (∼55%) (Fig. 2*D*), but remained at this high level throughout further development (Fig. 2 *C* and *D*). Thus, PSD-95 is required for the experience-dependent maturation of excitatory synapses onto pyramidal cells after eye opening.

Silent synapses are unsilenced on insertion of AMPARs, a process accompanied by an increase in the AMPAR/NMDAR (A/N) ratio. Accordingly, in the L4-to-L2/3 pathway of WT mice, the A/N ratio of pyramidal neurons increased from 1.4 on P25–30 to 2.2 on P60–70 (Fig. 2 *E* and *F*), whereas the A/N ratio was 1.0 in P25–30 PSD-95 KO mice and remained low on P60–70 (Fig. 2 *E* and *F*). Thus, the preservation of a juvenile A/N ratio also indicates that more excitatory V1 synapses onto pyramidal neurons remain in an immature state in adult PSD-95 KO mice.

PSD-95 Protein Levels in V1 Increase During the Critical Period for ODP. Because silent synapse numbers in PSD-95 KO compared with WT mice were not different before eye opening, we determined the developmental profile of PSD-95 protein levels in V1 of WT mice to identify the onset of PSD-95 protein expression. We isolated a crude synaptosomal protein fraction (P2) from V1 of WT mice at time points before eye opening (P9 and P11), after eye opening (P14 and P19), and at the beginning (P25) and end (P38) of the CP, and normalized them to the levels in adult mice (P90; Fig. 3). Although protein levels of mortalin, which we used as a loading control, did not change between the different time points analyzed, PSD-95 levels increased between eye opening and the beginning of the CP to reach ∼80% of adult levels at the end of the CP (Fig. 3*A*). In WT mice before eye opening, PSD-95 protein levels were below 10% of adult levels, indicating that ∼50% of synapses matured largely independent of PSD-95. This result is consistent with the similar fractions of silent synapses in WT and PSD-95 KO mice before eye opening. Furthermore, the increase of PSD-95 protein levels parallels the progressive maturation of silent synapses. Each of the active zone marker Munc13-1 and the NMDA receptor subunit GluN1 doubled from about 50% of adult levels to adult

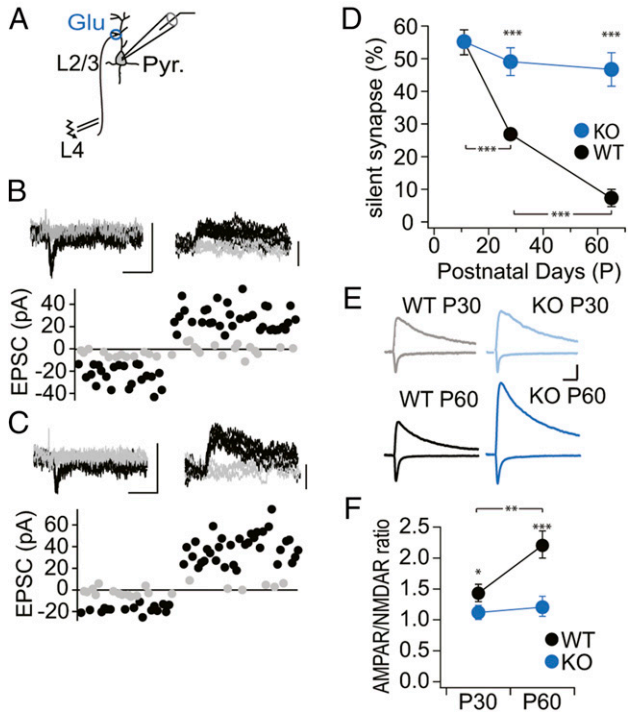

Fig. 2. Impaired developmental maturation of glutamatergic synapses in the visual cortex of PSD-95 KO mice. (*A*) Schematic drawing of the electrophysiological recording configuration in slices of the binocular segment of mouse V1. Pyramidal neurons (Pyr.) in L2/3 were patched in voltage-clamp mode, and synaptic afferents were stimulated extracellularly in L4. (*B* and *C*) Sample traces of EPSCs with minimal stimulation of P60 WT (*B*) and KO (*C*) mice to record unitary responses (*Upper*) and analysis of the peak values of AMPA receptor EPSCs, recorded at $V_h = -60$ mV (downward deflection) or composite glutamate receptor EPSCs, recorded at $V_h = +40$ mV (upward deflection) of successes (black) and failures (gray) of individual EPSCs. (Scale bar for *B*, *C*, and *E*, 20 ms and 50 pA.) (*D*) Summary graph of percentage of silent synapses [$F_{ag(2,14)} = 35.77$, $P < 0.001$; $F_{gt(1,14)} = 58.35$, $P < 0.001$; WT P10, n/m = 10/3; KO P10, n/m = 10/3; WT P30, n/m = 15/4; KO P30, n/m = 8/3; WT P60, n/m = 14/4; KO P60, n/m = 11/3; WT P10 vs. KO P10, KO P10 vs. KO P30, KO P30 vs. KO P60, KO P10 vs. KO P60; all $P > 0.05$]. (*E*) Sample traces of EPSCs were recorded at $V_h = -60$ mV and $V_h = +40$ mV from WT controls (P20–30/P60–70 in gray/black) and PSD-95 KO mice (P20–30/P60–70 in light blue/blue). (*F*) Summary graph of AMPA/NMDA receptor EPSC ratios [$F_{ag(1,10)} = 7.18$, $P < 0.05$; $F_{gt(1,10)} = 45.97$, $P < 0.001$; WT P30, n/m = 19/5; KO P30, n/m = 19/3; WT P60, n/m = 14/3; KO P60, n/m = 13/3: KO P30 vs. KO P60; $P > 0.05$]. $*P < 0.05$; $**P < 0.01$; $***P < 0.001$. Values in Table S2.

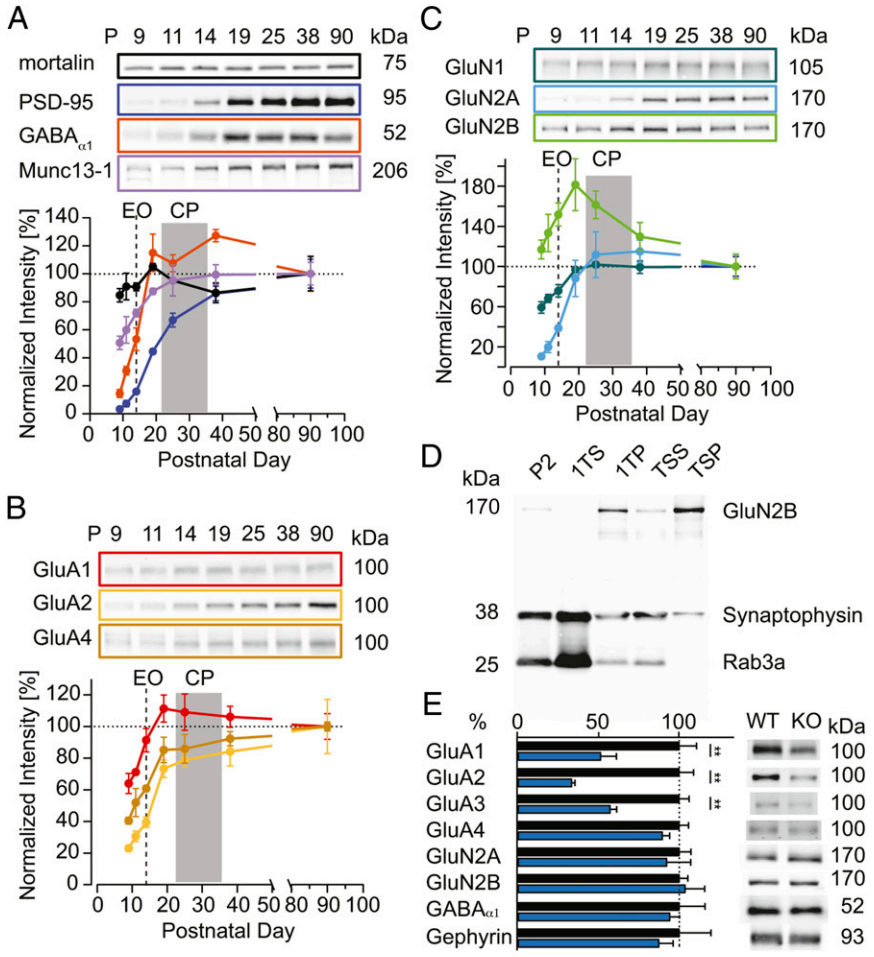

Fig. 3. Developmental changes in V1 of PSD-95 associated proteins and changes in synaptic protein composition in adult PSD-95 KO mice. (*A*–*C*) Developmental profile of synaptic proteins from crude synaptosomal fractions from V1 of WT mice (10–30 μg protein per lane). Sample blots are illustrated on top of each panel for the indicated proteins, and quantified protein levels, normalized to the adult levels at P90, are plotted against the postnatal day (P). $n = 4$–5 (mice). CP, critical period; EO, eye opening. (*D*) Sample blot for the characterization of the subcellular fractionation procedure; 10 μg of protein fraction loaded per lane. (*E*) Summary graph of quantified protein levels in PSD (TSP) fraction for adult WT (black) and PSD-95 KO mice (blue) (*Right*: sample blot). Band signal intensities were normalized to average signal of WT samples. $n = 5$ (mice). $^{**}P < 0.01$. Values in Table S3.

levels before the onset of the CP, indicating an increase in the size, and/or number of excitatory synapses after eye opening (Fig. 3 *A* and *C*). Similar to PSD-95, the protein levels of the NMDA receptor subunit GluN2A accumulated after eye opening (Fig. 3*C*). In contrast, the protein levels of GluN2B were high before eye opening with similar levels as in adult mice and peaked at the beginning of the CP (Fig. 3*C*), a result consistent with a specific role of GluN2B in CP plasticity. The GABA-A receptor subunit α1 showed the steepest increase from eye opening to the onset of the CP, consistent with the maturation of parvalbumin-positive interneurons at the beginning of the CP (42). The AMPA receptor subunits GluA1, GluA2, and GluA4 showed a parallel developmental profile with GluA1, reaching adult levels already at the beginning of the CP (Fig. 3*B*). Parallel to the maturation of silent synapses, the levels of GluA2 increased to adult levels until after the CP. In conclusion, these data are consistent with an exclusive role of PSD-95 in the experience-dependent maturation of synapses after eye opening and a change in the synaptic subunit composition of both AMPA and NMDA receptors during V1 development.

AMPA Receptor Subunits of Excitatory Neurons Are Reduced in Synaptic Protein Fractions of PSD-95 KO Mice. To determine which types of synaptic AMPA receptors were inserted in PSD-95–dependent unsilencing of silent synapses and whether other changes in synaptic receptor composition occurred, we quantified synaptic levels of specific AMPA receptor subunits and their scaffolds in the cortex of adult PSD-95 KO and WT mice. Using subcellular fractionation procedures, we enriched for cortical PSD fractions (TSP) (Fig. 3*D* and Fig. S2). The NMDA receptor subunit GluN2B was enriched in the fractionation procedure, whereas the synaptic vesicle proteins synaptophysin and Rab3a were strongly reduced, consistent with an enrichment of PSD proteins in TSP. When quantified, the protein levels of NMDA receptor subunits GluN2A and GluN2B were similar to that in WT mice (Fig. 3*E*). In contrast, in PSD-95 KO mice, the levels of the AMPA receptor subunits GluA1, GluA2, and GluA3 were ∼50% of that in WT mice, whereas levels of GluA4, which might be primarily expressed in inhibitory neurons (43), were not changed (Fig. 3*E*). These biochemical results indicate a lack of synaptic recruitment of all three major AMPA receptor subunits in developing cortical synapses in PSD-95 KO mice. Thus, there is a specific reduction of AMPA receptors but not NMDA receptors in PSD-95 KO mice. The reduction of AMPA receptor numbers by ∼50% indicates that in PSD-95 KO mice the transmitting synapses contain normal levels of AMPA receptors, whereas the silent synapses are devoid of AMPA receptors. Furthermore, the unaltered number of NMDA receptors in the PSD indicates that the NMDA receptor excitatory postsynaptic current (EPSC) is a valid marker for normalization of synaptic responses.

Development of Local Inhibitory Tone onto L2/3 Pyramidal Neurons Is Normal in PSD-95 KO Mice. Developmental strengthening of local inhibitory circuits contributes to the termination of the critical period for ODP (17, 44–46), and experimental reduction of the inhibitory tone partially restores ODP in older rodents (47–50). Thus, it is possible that the preserved juvenile-like ODP in adult PSD-95 KO mice was the result of a reduction in inhibitory tone. This reduction is, however, not likely. Quantification of PSD

proteins showed that several key markers of inhibitory synapses including gephyrin, the scaffolding protein of inhibitory synapses, and the $GABA_A$ receptor subunit $GABA_AR$-α1, a subunit that is particularly enriched in inhibitory synapses of PV-positive (+) interneurons to pyramidal cells, were not reduced in adult PSD-95 KO mice (Fig. 3*E*) (51).

Although our biochemical results are consistent with an unaltered inhibitory synaptic transmission in PSD-95 KO mice, it is possible that PSD-95 KO reduces the inhibitory tone indirectly by altering the excitatory drive to inhibitory neurons. To address this possibility, we measured the inhibitory tone in pyramidal neurons in the local L4 to L2/3 circuit (Fig. 4*A*). We used NMDAR EPSCs, which are independent of the expression level of PSD-95 (52, 53), to normalize AMPAR EPSCs and $GABA_A$ receptor-mediated inhibitory postsynaptic currents (IPSCs). To quantify all three synaptic components in isolation, we used a combination of holding potentials at the respective reversal potentials of other receptors and pharmacological isolation. The AMPAR component was isolated by clamping the neuron at the reversal potential of the $GABA_A$ receptor ($V_h = -72$ mV) when also NMDARs are blocked by Mg^{2+}. Next, we isolated the $GABA_A$ receptor IPSCs by clamping the neuron at the reversal potential ($V_h = 0$ mV) of both glutamate receptors, and finally we isolated the NMDAR EPSCs by clamping the neuron at positive potentials ($V_h = +40$ mV) to remove its Mg^{2+} block and by pharmacologically inhibiting AMPAR and $GABA_A$ receptor function (Fig. 4*B*). We used 2,3-dioxo-6-nitro-1,2,3,4-tetrahydrobenzo[*f*]quinoxaline-7-sulfonamide to inhibit AMPARs in a subset of recordings to prevent disynaptic stimulation of IPSCs and determined the fraction of direct GABAergic input on layer 2/3 pyramidal neurons (Fig. 4*A*). We found that ∼70% of recorded IPSCs were indirect, relying on the activation of upstream excitatory neurons. The remaining ∼30% were monosynaptic from directly stimulated GABAergic fibers originating likely from L4 (Fig. S3). In WT mice, the A/N ratio increased by ∼40% (from 0.8 to 1.2) from P25–30 to P60–70 (Fig. 4*C*). In contrast, in both P25–30 and P60–70 PSD-95 KO mice, the A/N ratio was ∼0.7 and thus was lower than that in WT P60–70 mice but similar to that in WT P25–30 mice (Fig. 4*C*). The results are consistent with our initial results showing impaired excitatory synapse maturation on L2/3 pyramidal neurons in PSD-95 KO mice (Figs. 2 and 3). In WT mice, the GABA/NMDA receptor ratio increased by ∼80% from P25–30 to P60–70 (Fig. 4*D*), consistent with the typical developmental increase of the GABAergic tone. In PSD-95 KO mice, a similar developmental increase by ∼80% of the GABA/NMDAR ratio was observed (Fig. 4*D*).

Because the majority (∼70%) of the GABAergic currents resulted from disynaptic stimulation (Fig. S3), excitatory synapses on GABAergic interneurons substantially contributed to the GABAergic tone. Furthermore, PSD-95 is expressed in PV+ interneurons, the interneuron subtype responsible for most feed forward and feedback inhibition in L2/3 (54, 55). However, it has not yet been experimentally tested whether excitatory synaptic strength on GABAergic neurons depends on PSD-95. To address this question, we measured the A/N ratio and estimated the strength of excitatory synapses onto L2/3 PV+ interneurons (Fig. 4*E*). We used a PV+ reporter mouse line (*Materials and Methods*) crossed with the PSD-95 KO mouse line to identify PV+ interneurons by their yellow fluorescence (Fig. S4). In PV+ interneurons of WT P60–70 mice, the A/N ratio was more than sevenfold higher than in pyramidal neurons, a property, which is typical for PV+ interneurons. In PV+ interneurons of PSD-95 KO mice, the A/N ratio was similar to that of WT mice (Fig. 4*G*). To test AMPAR function more directly, we recorded miniature (m)EPSCs of the L2/3 PV+ interneurons of age-matched WT and PSD-95 KO mice in the critical period (Fig. S5). Both the mEPSC amplitude and the frequency of events were similar between the two genotypes (Fig. S5), indicating a similar number

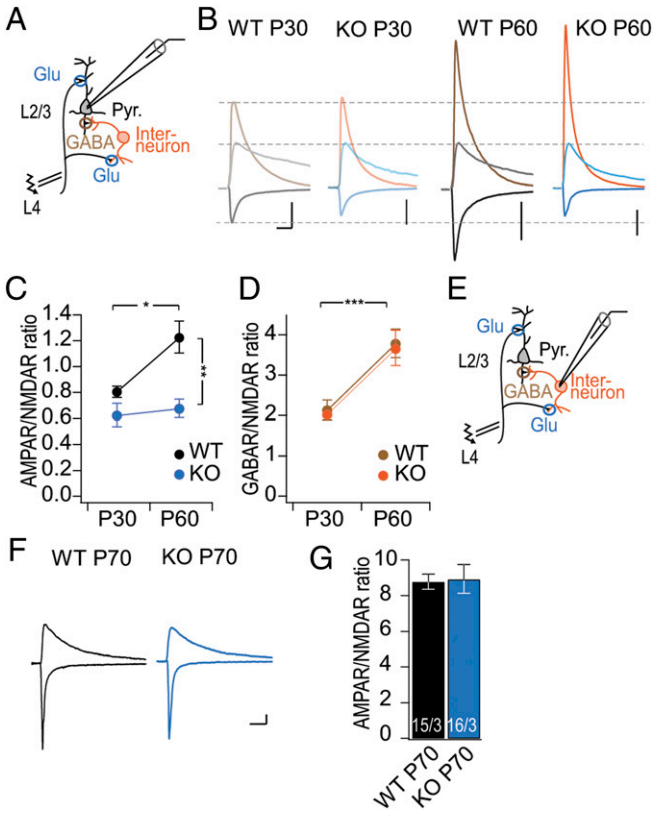

Fig. 4. Local inhibitory tone was normal in adult PSD-95 KO mice. (*A*) Schematic drawing of the electrophysiological recording configuration, similar to Fig. 2. Local interneurons are excited by the glutamatergic afferents (Glu) and synapse onto Pyr (GABA). (*B*) Sample traces of synaptic responses from L2/3 pyramidal neurons. Synaptic responses were separated into different components by clamping the neurons at the other receptors reversal potentials and specific antagonists. AMPA receptor EPSCs were recorded at the equilibrium potential of Cl^- at $V_h = -72$ mV (downward deflected traces in gray/black for P30/P60 WT and in light blue/dark blue for P30/P60 PSD-95 KO). GABA receptor IPSCs were recorded close to the reversal potential of glutamate receptors at $V_h = 0$ mV (upward deflected traces in light brown/brown for P30/P60 WT and in light orange/dark orange for P30/P60 PSD-95 KO mice). NMDA receptor EPSCs were recorded at $V_h = +40$ mV in the presence of the AMPA receptor blocker NBQX (10 μM) and GABA-A receptor blocker picrotoxin (50 μM; upward deflected traces in light gray/gray for P30/P60 WT and in light blue/dark blue for P30/P60 PSD-95 KO). (Scale bars, 20 ms and 200 pA.) (*C* and *D*) Summary graphs of the AMPA/NMDA receptor (*C*) and GABA/NMDA receptor ratios (*D*) (color code as in *B*). [*C*: $F_{ag(1,10)} = 6.22$, $P < 0.05$; $F_{gt(1,10)} = 18.17$, $P < 0.01$; WT P30, n/m = 16/4; WT P60, n/m = 16/4; KO P30, n/m = 17/3; KO P60, n/m = 14/3; KO P30 vs. KO P60, $P > 0.05$; and *D*: $F_{ag(1,10)} = 32.75$, $P < 0.001$; $F_{gt(1,10)} = 0.18$, $P = 0.68$; WT P30, n/m = 16/4; WT P60, n/m = 16/4; KO P30, n/m = 17/3; KO P60, n/m = 14/3; WT P60 vs. KO P60; $P > 0.05$.] (*E*) Schematic drawing of recording configuration for monosynaptic stimulation of interneuron. (*F*) Sample traces of synaptic responses from L2/3 PV+ interneurons with AMPAR EPSCs recorded at $V_h = -60$ mV and composite AMPA-NMDAR EPSCs at $V_h = +40$ mV of indicated genotype and age. (*G*) Summary graphs of the AMPA/NMDA receptor ratio for PV+ interneurons (WT P60 vs. KO P60, $P = 0.89$). Number of cells/mice in the foot of the bar. *$P < 0.05$; **$P < 0.01$; ***$P < 0.001$. Values in Table S4.

of AMPAR-containing synapses and/or release probability and, on average, a similar amount of AMPA receptor-mediated current per synapse. These data reveal that maturation of excitatory synapses onto PV+ interneurons, unlike in L2/3 pyramidal neurons, was not critically regulated by PSD-95. Thus, KO of PSD-95 does not affect excitatory synaptic transmission onto PV+ interneurons and does not exert an indirect effect on the GABAergic tone from these interneurons to pyramidal neurons.

To test the potential influence of the inhibitory tone on ODP in vivo, we next used a pharmacological manipulation. Diazepam was previously used to increase the GABAergic tone in pre-critical period mice to trigger the onset of the CP for ODP and to block restored plasticity after reduction of inhibition in older rodents (17, 44, 48, 49). Whereas diazepam treatment during the 7-d MD completely blocked ODP in adult (P80–106) WT mice (Fig. 1 *G* and *H*), this treatment did not abolish ODP in age-matched PSD-95 KO mice (WT vs. KO, $P < 0.001$). Thus, the life-long preservation of juvenile-like ODP in PSD-95 KO mice is not likely to be mediated by reductions in inhibitory tone but rather by immature excitatory synapses onto pyramidal neurons.

PSD-95 Stabilizes AMPA Receptors in Mature Synapses. To further test causality between PSD-95 manipulations, pyramidal neuron synaptic maturation, and the closure of the critical period, we manipulated PSD-95 levels conditionally. We achieved this manipulation via adeno-associated viral vector (AAV)-mediated gene transfer and expressed a PSD-95–targeting shRNA (sh95), which reduced the protein expression of PSD-95 by up to ∼90% in dissociated neuronal cultures (Fig. 5*A*) (56). We stereotactically injected low doses of the AAV-sh95 into the visual cortex of WT mice on P0 to achieve sparse transduction rates. The AAV-sh95–expressing mice were then analyzed at P30–33 and P60–70, time points at which we had measured the properties of excitatory synapses in V1 pyramidal neurons and ODP in the above experiments (Figs. 1 and 2). In sh95-expressing neurons, the A/N ratio at P30–33 and P60–70 was ≤1 and thus was smaller than nontransduced control neurons (Fig. 5 *C* and *D*). In sh95-expressing neurons, the A/N ratio did not change over development, whereas in nontransduced control neurons, a developmental increase was observed (Fig. 5 *C* and *D*). AAV manipulation as such had no influence on the A/N ratio, as the A/N ratio of nontransduced control cells and neurons transduced with a control viral vector were similar (Fig. 5*D*). Importantly, the A/N ratio of the single manipulated neurons was similar to that of age-matched PSD-95 KO neurons (sh95 P30–33 vs. KO P25–30, $P = 0.45$; sh95 P60–70 vs. KO P60–70, $P = 0.70$).

To test whether the A/N ratio reduction in the sh95 neurons was due to silent synapses, we quantified their numbers with the minimal stimulation assay. The fraction of silent synapses at P30–33 was more than twofold bigger in sh95 neurons than control neurons (Fig. 5*G*). The sh95 values were similar to the age-matched fraction of silent synapses in PSD-95 KO mice (sh95 P30–33 vs. KO P25–30, $P = 0.86$). These results show that the impairment of synaptic maturation caused by reduced PSD-95 expression was cell autonomous and not a secondary effect of network alterations.

To test whether PSD-95 is required for the stabilization of the matured silent synapses, we injected AAV-sh95 into the V1 of WT mice at P40, thus after the end of the CP, and measured the number of silent synapses at P60–70. In control neurons, the fraction of silent synapses was low and similar to that in WT mice (ctr. vs. WT, $P = 0.20$). In contrast, AAV-sh95 pyramidal neurons expressed more silent synapses (Fig. 5*J*). The fraction of silent synapses reinstated with AAV-sh95 after P60 was similar to the fraction of silent synapses in PSD-95 KO mice at a comparable age (sh95 vs. 95KO, $P = 0.83$). Thus, PSD-95 was also required to stabilize matured synapses, and later loss of PSD-95 could reinstate the silent state. The similar value of ∼50% for the fraction of silent synapses indicates that the PSD-95–dependent maturation occurred in a subpool of synapses, which require PSD-95 both for maturation and stabilization of the matured state.

To test the reinstatement of the juvenile-like ODP with sh95 after maturation at an even later time point, we injected WT mice with AAV-sh95 in V1 at P60. We measured the A/N ratio at P80–90. In control neurons, the A/N ratio was similar to that at P60–70, indicating that excitatory synapse maturation was completed before P60–70 (Fig. 5*K*). In contrast, in sh95-expressing neurons, the A/N ratio was ∼1, similar to the A/N ratio with AAV-sh95 expression starting at P0 and lower than that of the nontransduced control neurons (Fig. 5*K*). Thus, similar to the P40 transduction with AAV-sh95, the P60 transduction reinstated juvenile features in V1 synapses. Both the fraction of silent synapses and the A/N ratio were similar to that when PSD-95 was absent from synapses at birth, indicating that synapses, which depend on PSD-95 during experience-dependent maturation from eye opening onward, also are the ones losing the mature state if PSD-95 is removed later. These data indicate that at least two subpools of synapses are present in V1: one that depends on PSD-95 function for maturation and one that does not.

V1-Specific Reduction of PSD-95 Expression After Maturation Restores Juvenile-Like ODP. We then explored whether PSD-95 manipulations restricted to the visual cortex were sufficient to prevent the closure of the CP for ODP and whether the PSD-95–dependent rejuvenation of the excitatory synapses in V1 can restore CP-like ODP in adult WT mice. In P0 mice, we silenced PSD-95 expression selectively in the visual cortex of both hemispheres with AAV-sh95 and tested ODP at ∼P80. In mice with V1-specific PSD-95 silencing, a 4-d MD induced an OD shift toward the open eye, whereas in age-matched control mice, injected with AAV-GFP, ODP was absent after a 4-d MD (Fig. 6 *A*–*D*). The OD shift of mice with silenced PSD-95 in the visual cortex was similar in magnitude as in PSD-95 KO mice (Fig. 1). This shift was mediated by a reduction of deprived eye responses (Fig. 6 *B* and *D*). In contrast, in GFP control mice after a 4-d MD, V1 activity was still dominated by the deprived, contralateral eye (Fig. 6 *A*, *C*, and *D*). This result is consistent with previous observations that a 4-d MD is not sufficient to induce ODP in mice beyond the CP (38).

Callosal projections critically contribute to the expression of ODP in rodent V1 (57). Knockdown of PSD-95 in one or both hemispheres allowed us to test the requirement of excitatory synapse maturation in either V1 for juvenile-like ODP. In P0 WT mice, we silenced PSD-95 expression selectively with AAV-sh95 contralateral or ipsilateral to the deprived eye and imaged the contralateral cortex to measure ODP. After a 4-d MD at ∼P80, an OD shift was only induced when PSD-95 was silenced in the visual cortex contralateral to the deprived eye (recorded hemisphere, left) (Fig. 6 *C* and *D*). In contrast, silencing of PSD-95 in the cortex ipsilateral to the deprived eye (right hemisphere) did not preserve juvenile-like ODP in the imaged left cortex. Thus, impaired PSD-95–dependent maturation of V1 networks contralateral to the deprived eye is sufficient to preserve juvenile-like ODP in this hemisphere, indicating that the expression of ODP and thus the resulting reduction in contralateral eye responses is confined to the contralateral cortex.

We then tested whether reversing the maturation of excitatory synapses in V1 via PSD-95 silencing restores juvenile-like ODP in adult WT mice. At the end of the critical period (P40), we transduced V1 of WT mice bilaterally with AAV-sh95 (Fig. 6*I*). Whereas control mice transduced with AAV-GFP did not show ODP after a 4-d MD at ∼P80 (Fig. 6 *E* and *G*), juvenile-like ODP was restored in AAV-sh95–expressing mice (Fig. 6 *F*–*H*) and was accompanied by a reduction of deprived eye responses (Fig. 6 *F* and *H*). Thus, PSD-95 regulates maturation of excitatory synapses in a cell autonomous manner and is required both for the maturation and stabilization of the matured state. Knockdown of PSD-95 in the visual cortex contralateral to the deprived eye at P0 was sufficient to preserve juvenile-like ODP and sh95-based rejuvenation of excitatory synapses in V1 after the critical period restored juvenile-like ODP.

Neural Circuit Changes Are Less Stable in PSD-95 KO Mice. Long-term synaptic potentiation (LTP) is enhanced in the hippocampus of PSD-95 KO mice (58). However, potentiated spines (after LTP

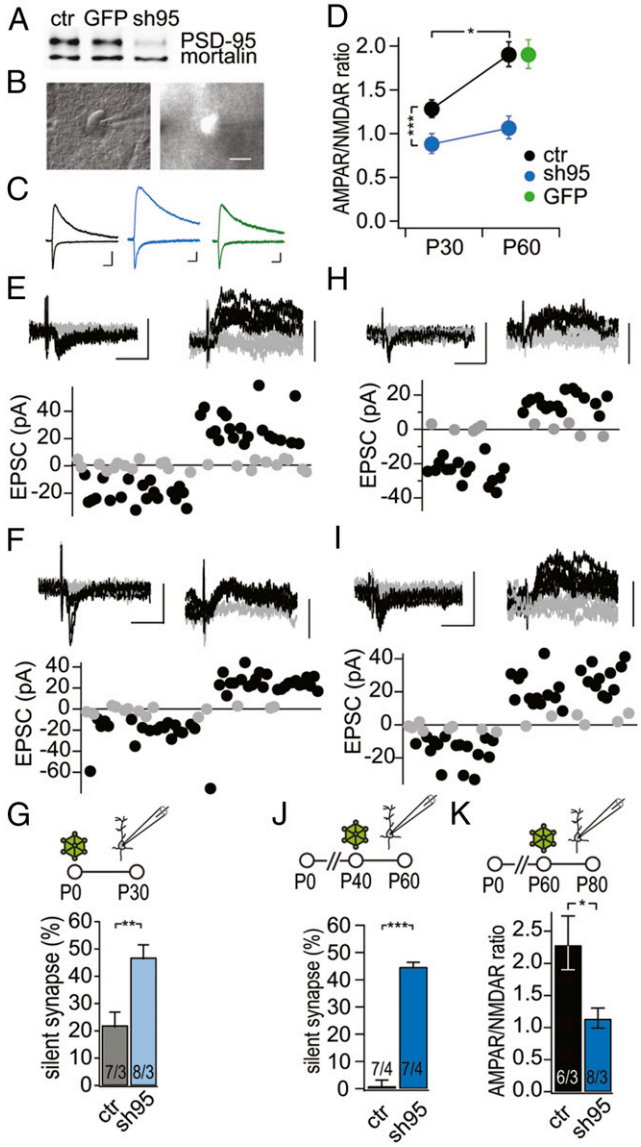

Fig. 5. PSD-95 controls both the maturational unsilencing and the stabilization of the matured state of synapses onto pyramidal neurons. (*A*) Knockdown efficiency of AAV-sh95 tested in dissociated mouse neuronal cultures by immunoblotting. PSD-95 protein levels were reduced by ∼90% in AAV-sh95 transduced cultures, whereas AAV-GFP had no effect on PSD-95 protein levels. Mortalin was probed as a loading control. (*B*) Sample image of a patched AAV-sh95–transduced V1 pyramidal neuron with differential interference contrast imaging (*Left*) and fluorescence imaging (*Right*). (Scale bar, 10 μm.) (*C*) Sample traces of EPSCs were recorded at V_h = –60 mV (downward deflection) and V_h = +40 mV (upward deflection) from nontransduced control (black), AAV-sh95–transduced neuron (blue) and AAV-GFP transduced neuron (green). (Scale bar, 20 ms and 50 pA.) (*D*) Summary graph of AAV-sh95 transduced neurons at P0, recorded on P30–33 and P60–70 [$F_{ag(1,40)}$ = 7.71, $P < 0.01$; $F_{gt(1,40)}$ = 20.78, $P < 0.001$; control P30–33, n/m = 8/3 vs. sh95 P30–33, n/m = 8/3, $P > 0.05$; control P60–70, n/m = 17/6; sh95 P60–70, n/m = 11/3; sh95 P30–33 vs. sh95 P60–70, $P > 0.05$]. AAV-GFP transduced neurons on P0, recorded on P60–70 (GFP P60–70, n/m = 19/5 vs. control P60–70, $P = 0.99$). (*E* and *F*) Sample traces of EPSCs with minimal stimulation. AAV-sh95 was injected on P0 into the visual cortex of WT mice and nontransduced control (*E*) and AAV-sh95 transduced pyramidal neurons (*F*) recorded on ∼P30. (*G*) Summary graph of WT mice, injected with AAV-sh95 on P0 and sh95-transduced and control neurons analyzed on P30–33. (*H* and *I*) Sample traces of EPSCs with minimal stimulation. AAV-sh95 was injected on P40 into V1 and control (*H*) and AAV-sh95–transduced pyramidal neurons (*I*) recorded on P60–70. (*J*) Summary graph of control or transduced pyramidal neurons. AAV-sh95 was injected on P40 into V1 and analyzed on P60–70. (*K*) AMPA/NMDA receptor EPSC ratios of AAV transduced neurons at P60, recorded at P80–90. (*G*, *J*, and *K*) Number of cells/mice in the foot of the bar. *$P < 0.05$; **$P < 0.01$; ***$P < 0.001$. Values in Table S2.

induction) are highly labile in PSD-95–deficient neurons (33), indicating that synaptic maturation during the fine-tuning of neuronal response properties in the critical period is unstable and only transient in the KO mice. To test whether cortical plasticity in PSD-95 KO mice is more transient, we performed a modified ODP paradigm. After a 7-d MD, the initially deprived eye was reopened, and visual cortical activity was imaged 2 or 4 d after reopening. In adult WT mice, the OD shift was maintained 2 d after reopening (7-d MD vs. 2-d reopen, $P = 0.18$) and restored only after 4 d (Fig. 7). In contrast, in PSD-95 KO mice, 2 d of reopening was sufficient to induce a recovery of OD of the previously deprived eye (Fig. 7). Thus, the plastic changes induced in V1 of adult PSD-95 KO mice were more transient and faster to be reversed than in WT mice, indicating that synaptic changes during experience-dependent network refinements cannot be consolidated, and functional properties of neurons may not be stabilized without PSD-95. This notion is further supported by our finding that silent synapses remain abundant in adult PSD-95 KO mice and thus are not integrated as mature, transmitting synapses into the cortical network, a process normally occurring during cortical development.

Discussion

Silent synapses are substrates for activity-dependent strengthening of synaptic transmission at excitatory synapses in the hippocampus and cortex (23, 24). They are abundant at the beginning of experience-dependent cortical network refinement, which is characterized by progressive dendritic spine stabilization and decreased spine elimination (11, 12). This refinement is thought to result in functionally optimized neural connections. During early synaptic sensory pathway development, decreasing numbers of silent synapses parallel the susceptibility for LTP (40), a cellular mechanism that may underlie the experience-dependent strengthening and maturation of synapses (10). In agreement with previous studies, we show that at eye opening when visual experience starts, ∼50% of L4 to L2/3 V1 synapses are silent (Fig. 2) (59), which end with a remaining 5% and less of silent synapses in adult mice (Fig. 2) (25).

Here, we provide evidence that a PSD-95–based mechanism governs the gradual cortical development and termination of CPs. Our conceptual model integrates synapse stabilization during cortical neural network refinement with the closure of CPs. Several of our results support the causality between PSD-95–dependent synapse maturation and the closure of the CP for juvenile ODP.

First, experience-dependent maturation of silent synapses was absent in PSD-95 KO mice (Fig. 2), and concurrently, critical period-like ODP was preserved lifelong in PSD-95 KO mice (Fig. 1). PSD-95 is absolutely required for the experience-dependent reduction of silent synapses; as in PSD-95 KO mice, the fraction of silent synapses remained at the high eye opening level throughout development and thus with 100% penetrance (Fig. 2). It is known that silent synapse numbers decrease during critical periods (13, 25). Our results show the reverse correlation that lack of silent synapse maturation correlates with the persistence of juvenile-like ODP in V1, indicating that by preventing silent synapse maturation, the termination of the CP for juvenile-like ODP is prevented as well. Similarly, dark rearing from birth preserves juvenile-like ODP (60) and results in an elevated number of silent synapses (25). However, the retardation of silent synapse maturation and critical period closure have not been causally linked. Instead, given that dark rearing profoundly influences the properties of neural circuits, including excitatory/inhibitory balance and metaplasticity (delaying the NMDA receptor subunit switch from GluN2B to GluN2A), other cellular mechanisms have been favored (61–65). An impaired developmental NMDA receptor subunit switch is unlikely causal for the lack of CP closure in PSD-95 KO mice: Although in young PSD-95 KO mice more synaptic GluN2B-containing NMDA receptors are

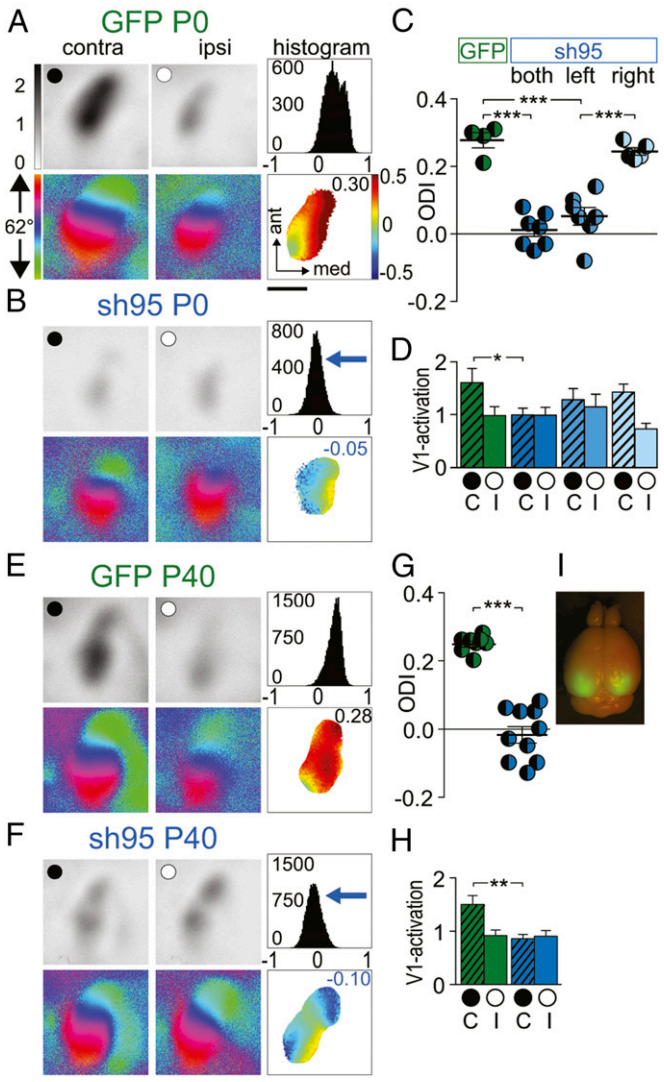

Fig. 6. PSD-95 controls the closure of the critical period for juvenile ocular dominance plasticity. Optically imaged activity maps (*A*, *B*, *E*, and *F*) and their quantification (*C*, *D*, *G*, and *H*) in V1 of AAV-GFP and AAV-sh95 mice transduced at P0 (*A*–*D*) and P40 (*E*–*H*). V1 recordings after a 4-d MD at >P80. Data displayed as in Fig. 1. (Scale bar, 1 mm.) ODIs (*C* and *G*) and V1 activation (*D* and *H*) after a 4-d MD in AAV-GFP–transduced mice at P0 (*C* and *D*) or P40 (*G* and *H*); AAV-sh95 transduced bilaterally at P0 (both; *A*, *C*, and *D*) or P40 (*E*, *G*, and *H*) or at P0 only contra- (left; *C* and *D*) or ipsilateral to the deprived eye (right; *C* and *D*) (GFP P0 vs. sh95 P0 right hemisphere, $P = 0.20$). (*D* and *H*) V1 activation elicited by stimulation of the contralateral (C) or ipsilateral (I) eye. (*I*) GFP fluorescence was illuminated in a perfusion fixed brain, which was transduced on P40 with AAV-sh95 and analyzed on P80 (see also confocal microscopy of slices in Fig. S6). $^*P < 0.05$; $^{**}P < 0.01$; $^{***}P < 0.001$. Values in Table S1.

present (35), the synaptic GluN2B levels are not altered in adult PSD-95 KO mice (56). Furthermore, in GluN2A KO mice, ODP is restricted rather than enhanced (36).

Second, to narrow down the locus where ODP is expressed, we performed a visual cortex-restricted knockdown of PSD-95, which impaired excitatory synapse maturation (Fig. 5) and preserved CP-like ODP into late adulthood (Fig. 6). This dependency was further substantiated by our result that reduction of PSD-95 in the visual cortex contralateral to the deprived eye was sufficient to preserve juvenile-like ODP after MD (Fig. 6). These results pinpoint the locus of expression of ODP to the contralateral V1 of the deprived eye rather than bilateral expression mechanisms, a locus of expression in upstream neurons of the visual pathway, or in other brain regions such as modulatory neurotransmitter systems.

Third, we directly tested our conceptual model that PSD-95–dependent silent synapse maturation marks the end of critical periods by knocking down PSD-95 in V1 after the end of the critical period for juvenile ODP. In support for the model, this manipulation reverted mature synapses to silent synapses (Fig. 5) and revealed critical period-like ODP (Fig. 6).

Fourth, our results highlight the essential role of excitatory synapses of pyramidal neurons in expressing juvenile-like ODP. In support of this notion, excitatory synapses onto PV+ interneurons and the inhibitory projection onto layer 2/3 pyramidal neurons were not altered in PSD-95 KO mice (Fig. 4). Furthermore, although pharmacological enhancement of inhibition in vivo prevented ODP in WT mice, it had no influence on juvenile-like ODP in PSD-95 KO mice (Fig. 1). Thus, glutamatergic synapses onto PV+ interneurons do not require PSD-95 for maturation, and the role of PSD-95 is rather specific for the developmental unsilencing of excitatory synapses onto pyramidal neurons. Importantly, the silent synapse-based ODP is largely independent of the inhibitory tone and thus contrasts the current view that increased intracortical inhibition is causal for the closure of CPs (26). Our results show that juvenile-like ODP cannot only persist but also be reinstated in the presence of high levels of intracortical inhibition, if silent synapse levels are high (Figs. 1, 2, and 6). Together, our findings highlight that the closure of the CP for juvenile-like ODP is caused by the maturation of excitatory synapses onto V1 pyramidal neurons, primarily due to experience-dependent unsilencing of silent synapses, in which PSD-95 is required for the stabilization of AMPA receptors in the unsilenced mature synapses.

Importantly, ∼50% synapses matured independently of PSD-95 already before eye opening and thus before the developmental increase of PSD-95 protein expression paralleling silent synapse maturation (Fig. 3) (32). It appears that at least two subpopulations of synapses exist: one PSD-95 independent and potentially static and the other one plastic and requiring PSD-95 for experience-dependent maturation. This notion is supported by two lines of evidence. First, we found that reducing PSD-95 either throughout development (Fig. 2), or after birth, or after synapses had already matured (Fig. 5) resulted in a similar ∼50% reduction in AMPAR EPSCs, more specifically in the reappearance of ∼50% silent synapses. This result is in agreement with previous studies in the hippocampus, which analyzed PSD-95 function in synaptic maturation by loss-of-function approaches in still-developing synapses and consistently showed a ∼50% reduction in AMPAR EPSCs (33, 35, 52, 53).

Second, loss-of-PSD-95 in excitatory synapses onto PV+ interneurons did not alter basal AMPAR function (Fig. 4 and Fig. S5). All four PSD-95 paralogs are expressed in PV+ V1 interneurons

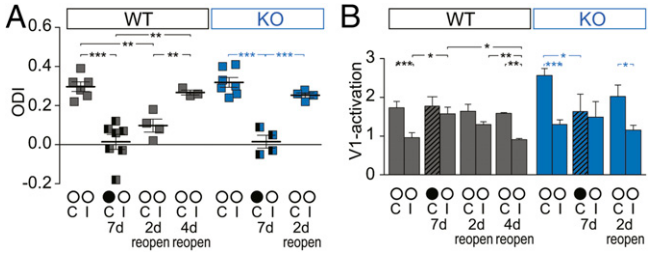

Fig. 7. MD-induced changes are less stable in V1 of adult PSD-95 KO mice. ODIs (*A*) and V1 activation (*B*) 2 or 4 d after reopening the formerly deprived eye (KO reopen 2-d C vs. KO <P110 7-d MD C, $P = 0.49$). Values of control WT and PSD-95 KO mice with and without 7-d MD are from Fig. 1. Layout as in Fig. 1. $^*P < 0.05$; $^{**}P < 0.01$; $^{***}P < 0.001$. Values in Table S1.

(55). Although we cannot rule out that AMPAR numbers are primarily regulated by PSD-95 paralogs in inhibitory neurons, this result further strengthens our conclusion that the prime function of PSD-95 is to regulate a subpopulation of dynamic synapses onto principal neurons by converting silent to mature synapses, a process typical for principal neuron but not interneuron development (66).

Our conceptual model integrates synapse stabilization during cortical network refinement with the closure of CPs. During these refinements, in experience-dependent processes, synapses will be either stabilized (10) or pruned (11, 12). Our model does not exclude an essential contribution of the inhibitory network in regulating critical period plasticity (15, 16, 67). Because thresholds for Hebbian plasticity are sculpted by inhibitory neurotransmission (68), it is very likely that a PSD-95–governed synaptic plasticity mechanism in silent synapse maturation acts in concert with the inhibitory circuitry to refine cortical networks during CPs. Importantly, our data show that the inhibitory tone is permissive in regulating juvenile ODP, as the duration of ODP is governed by the presence of silent synapses and is independent of the inhibitory tone.

Notably, the expression of the juvenile characteristics of ODP can be established through other mechanisms than silent synapses under certain experimental conditions. We showed that environmental enrichment can prolong and reinstate juvenile-like ODP, whereas the measured AMPA/NMDA receptor ratio was unchanged in V1 of adult enriched mice, and thus it is unlikely that generation of new silent synapses was induced (69). Thus, either different expression mechanisms could cause the same system level read-out with depression of deprived eye responses or the expression mechanism is independent of the existence of silent synapses. It is also important to note that synaptic plasticity at different developmental time points likely serve different purposes. During CPs in early cortical development, functionally optimal synaptic connections are sculpted by experience. Silent synapses are ideally suited for this purpose, as these preexisting synapses can be stably integrated into the pathway if repeatedly recruited by activity, whereas they might be pruned if not. Later in life, learning is still possible and may rely on other plasticity mechanisms. However, specific sensory features, which are not learned during its CP, will not be acquired to the possible optimum (3, 26).

Previous studies have shown that absence of the Nogo-66 receptor or PirB extends ODP into adulthood (20–22). However, for Nogo-66, it needs to be tested whether it is the juvenile form and whether PirB plays a role in the adult form of ODP (22). These proteins influence both structural plasticity of the extracellular matrix and axon sprouting, as well as long-term synaptic plasticity. A molecular or functional interaction of these proteins with PSD-95 is unknown. Notably, disintegration of the extracellular matrix can reactivate ODP (18). Thus, both PSD-95 and PirB might act via different mechanisms to stabilize synapses. Nevertheless, experience-dependent silent synapse maturation to terminate critical periods provides an attractive mechanism how synaptic unsilencing, synaptic plasticity, and cortical plasticity are linked for neural network refinements during development. Further experiments will be required to clarify the role of Nogo-66 receptor and PirB for experience-dependent maturation of silent synapses, as well as the interplay between inhibitory circuit maturation and unsilencing of excitatory synapses (48, 68).

In conclusion, we link PSD-95 function to experience-dependent maturation of silent synapses in the CP for ODP, demonstrating an essential function of silent synapses in neural network refinement and presumably their conversion into transmitting synapses as the terminating event for CPs. The time window for ODP thus stays open despite the normal developmental increase of local inhibitory tone in PSD-95 KO mice and can be reopened when silent synapses are reinstated with acute knockdown of PSD-95 in V1 in adult mice. This result shows that ODP can persist in the presence of high levels of inhibition, given additional plasticity substrates such as silent synapses. We propose that experience-dependent unsilencing of silent synapses constitutes an important general maturational process during CPs of cortical development of different functional domains and suggest an interplay with inhibitory circuits in regulating plasticity (68).

Materials and Methods

PSD-95 KO mice and PV+ reporter mice have been described previously (70–72). All procedures were performed by strictly following the procedures approved by the animal care and use committees and governmental agencies of the listed institutions.

Standard whole-cell voltage-clamp recordings and minimal stimulation procedures from coronal V1 slices were carried out using standard procedures as previously described (23, 24, 69). For AMPA/NMDA receptor ratios, the AMPA receptor component was measured as a peak value at $V_h = -60$ mV and the NMDA receptor component was measured at $V_h = +40$ mV at 60 ms after the AMPA receptor peak.

Visual acuity of the mice was assessed using the VWT, a visual discrimination task that is based on reinforcement learning (39). The right eye was deprived of vision for 4 or 7 d according to published protocols (28, 73). Mouse visual cortical responses were recorded through the skull using the imaging method developed by Kalatsky and Stryker and optimized for the assessment of OD plasticity by Cang et al. (73, 74). The experimenter was blinded for the genotype of the recorded mouse, and data were analyzed as detailed elsewhere (37, 73, 74). More details are described in *SI Materials and Methods*.

Data are represented as means ± SEM. For electrophysiological data, averages of ratios were calculated after logarithmic transformation and presented as back-transformed mean ± SEM. For statistical analysis, the two-way ANOVA test with a Bonferroni post hoc test was used for comparison between age (ag) and genotypes (gt) in an experimental group. Intergroup comparisons, Western blot, and VWT data were analyzed using a two-tailed *t* test with unequal variance. All intra- and intergroup comparisons of the imaging data were done by a two-tailed *t* test with Bonferroni correction. The levels of significance were set as $P < 0.05$; $P < 0.01$; and $P < 0.001$.

ACKNOWLEDGMENTS. We thank Drs. S. Arber, S. Grant, and H. Zeng for mouse lines; Dr. N. Brose for antibodies; Drs. N. Brose, L. White, and W. Xu for comments on the manuscript; S. Ott-Gebauer and M. Schink for excellent technical assistance; and Dr. K.-F. Schmidt for help with some of the experiments. This work was supported by the German Research Foundation through the Collaborative Research Center 889 "Cellular Mechanisms of Sensory Processing" [to S.L. (Project B5) and O.M.S. (Project B3)], and Grant SCHL592/4 (to O.M.S.), and Federal Ministry of Education and Research Grants 01GQ0921 (to S.K.S.) and 01GQ0810 (to S.L. and B.G.). The European Neuroscience Institute Göttingen is jointly funded by the Max-Planck Society and University Medicine Göttingen.

1. Zipursky SL, Sanes JR (2010) Chemoaffinity revisited: Dscams, protocadherins, and neural circuit assembly. *Cell* 143(3):343–353.
2. Feldman DE (2009) Synaptic mechanisms for plasticity in neocortex. *Annu Rev Neurosci* 32:33–55.
3. Espinosa JS, Stryker MP (2012) Development and plasticity of the primary visual cortex. *Neuron* 75(2):230–249.
4. Brainard MS, Doupe AJ (2002) What songbirds teach us about learning. *Nature* 417(6886):351–358.
5. Lorenz KZ (1958) The evolution of behavior. *Sci Am* 199(6):67–74, passim.
6. Johnson JS, Newport EL (1989) Critical period effects in second language learning: The influence of maturational state on the acquisition of English as a second language. *Cognit Psychol* 21(1):60–99.
7. Penhune VB (2011) Sensitive periods in human development: Evidence from musical training. *Cortex* 47(9):1126–1137.
8. Hertle RW, et al.; Pediatric Eye Disease Investigator Group (2007) Stability of visual acuity improvement following discontinuation of amblyopia treatment in children aged 7 to 12 years. *Arch Ophthalmol* 125(5):655–659.
9. Wang B-S, Sarnaik R, Cang J (2010) Critical period plasticity matches binocular orientation preference in the visual cortex. *Neuron* 65(2):246–256.
10. Ashby MC, Isaac JTR (2011) Maturation of a recurrent excitatory neocortical circuit by experience-dependent unsilencing of newly formed dendritic spines. *Neuron* 70(3):510–521.
11. Zuo Y, Lin A, Chang P, Gan W-B (2005) Development of long-term dendritic spine stability in diverse regions of cerebral cortex. *Neuron* 46(2):181–189.

12. Holtmaat AJGD, et al. (2005) Transient and persistent dendritic spines in the neocortex in vivo. *Neuron* 45(2):279–291.
13. Isaac JT, Crair MC, Nicoll RA, Malenka RC (1997) Silent synapses during development of thalamocortical inputs. *Neuron* 18(2):269–280.
14. Kirkwood A, Rioult MC, Bear MF (1996) Experience-dependent modification of synaptic plasticity in visual cortex. *Nature* 381(6582):526–528.
15. Kuhlman SJ, et al. (2013) A disinhibitory microcircuit initiates critical-period plasticity in the visual cortex. *Nature* 501(7468):543–546.
16. Morishita H, Hensch TK (2008) Critical period revisited: Impact on vision. *Curr Opin Neurobiol* 18(1):101–107.
17. Fagiolini M, et al. (2004) Specific GABAA circuits for visual cortical plasticity. *Science* 303(5664):1681–1683.
18. Pizzorusso T, et al. (2002) Reactivation of ocular dominance plasticity in the adult visual cortex. *Science* 298(5596):1248–1251.
19. Mataga N, Nagai N, Hensch TK (2002) Permissive proteolytic activity for visual cortical plasticity. *Proc Natl Acad Sci USA* 99(11):7717–7721.
20. McGee AW, Yang Y, Fischer QS, Daw NW, Strittmatter SM (2005) Experience-driven plasticity of visual cortex limited by myelin and Nogo receptor. *Science* 309(5744): 2222–2226.
21. Syken J, Grandpre T, Kanold PO, Shatz CJ (2006) PirB restricts ocular-dominance plasticity in visual cortex. *Science* 313(5794):1795–1800.
22. Djurisic M, et al. (2013) PirB regulates a structural substrate for cortical plasticity. *Proc Natl Acad Sci USA* 110(51):20771–20776.
23. Isaac JTR, Nicoll RA, Malenka RC (1995) Evidence for silent synapses: Implications for the expression of LTP. *Neuron* 15(2):427–434.
24. Liao D, Hessler NA, Malinow R (1995) Activation of postsynaptically silent synapses during pairing-induced LTP in CA1 region of hippocampal slice. *Nature* 375(6530):400–404.
25. Funahashi R, Maruyama T, Yoshimura Y, Komatsu Y (2013) Silent synapses persist into adulthood in layer 2/3 pyramidal neurons of visual cortex in dark-reared mice. *J Neurophysiol* 109(8):2064–2076.
26. Takesian AE, Hensch TK (2013) Balancing plasticity/stability across brain development. *Prog Brain Res* 207:3–34.
27. Hubel DH, Wiesel TN (1970) The period of susceptibility to the physiological effects of unilateral eye closure in kittens. *J Physiol* 206(2):419–436.
28. Gordon JA, Stryker MP (1996) Experience-dependent plasticity of binocular responses in the primary visual cortex of the mouse. *J Neurosci* 16(10):3274–3286.
29. Dräger UC (1978) Observations on monocular deprivation in mice. *J Neurophysiol* 41(1):28–42.
30. Sawtell NB, et al. (2003) NMDA receptor-dependent ocular dominance plasticity in adult visual cortex. *Neuron* 38(6):977–985.
31. Kaneko M, Stellwagen D, Malenka RC, Stryker MP (2008) Tumor necrosis factor-alpha mediates one component of competitive, experience-dependent plasticity in developing visual cortex. *Neuron* 58(5):673–680.
32. Yoshii A, Sheng MH, Constantine-Paton M (2003) Eye opening induces a rapid dendritic localization of PSD-95 in central visual neurons. *Proc Natl Acad Sci USA* 100(3): 1334–1339.
33. Ehrlich I, Klein M, Rumpel S, Malinow R (2007) PSD-95 is required for activity-driven synapse stabilization. *Proc Natl Acad Sci USA* 104(10):4176–4181.
34. Stein V, House DRC, Bredt DS, Nicoll RA (2003) Postsynaptic density-95 mimics and occludes hippocampal long-term potentiation and enhances long-term depression. *J Neurosci* 23(13):5503–5506.
35. Béïque J-C, et al. (2006) Synapse-specific regulation of AMPA receptor function by PSD-95. *Proc Natl Acad Sci USA* 103(51):19535–19540.
36. Fagiolini M, et al. (2003) Separable features of visual cortical plasticity revealed by N-methyl-D-aspartate receptor 2A signaling. *Proc Natl Acad Sci USA* 100(5):2854–2859.
37. Lehmann K, Löwel S (2008) Age-dependent ocular dominance plasticity in adult mice. *PLoS ONE* 3(9):e3120.
38. Sato M, Stryker MP (2008) Distinctive features of adult ocular dominance plasticity. *J Neurosci* 28(41):10278–10286.
39. Prusky GT, West PW, Douglas RM (2000) Behavioral assessment of visual acuity in mice and rats. *Vision Res* 40(16):2201–2209.
40. Rumpel S, Hatt H, Gottmann K (1998) Silent synapses in the developing rat visual cortex: Evidence for postsynaptic expression of synaptic plasticity. *J Neurosci* 18(21): 8863–8874.
41. Liu C-H, Heynen AJ, Shuler MGH, Bear MF (2008) Cannabinoid receptor blockade reveals parallel plasticity mechanisms in different layers of mouse visual cortex. *Neuron* 58(3):340–345.
42. Hensch TK (2005) Critical period plasticity in local cortical circuits. *Nat Rev Neurosci* 6(11):877–888.
43. Geiger JR, et al. (1995) Relative abundance of subunit mRNAs determines gating and Ca2+ permeability of AMPA receptors in principal neurons and interneurons in rat CNS. *Neuron* 15(1):193–204.
44. Hensch TK, et al. (1998) Local GABA circuit control of experience-dependent plasticity in developing visual cortex. *Science* 282(5393):1504–1508.
45. Sugiyama S, et al. (2008) Experience-dependent transfer of Otx2 homeoprotein into the visual cortex activates postnatal plasticity. *Cell* 134(3):508–520.
46. Jiang B, et al. (2010) The maturation of GABAergic transmission in visual cortex requires endocannabinoid-mediated LTD of inhibitory inputs during a critical period. *Neuron* 66(2):248–259.
47. Harauzov A, et al. (2010) Reducing intracortical inhibition in the adult visual cortex promotes ocular dominance plasticity. *J Neurosci* 30(1):361–371.
48. Morishita H, Miwa JM, Heintz N, Hensch TK (2010) Lynx1, a cholinergic brake, limits plasticity in adult visual cortex. *Science* 330(6008):1238–1240.
49. Maya Vetencourt JF, et al. (2008) The antidepressant fluoxetine restores plasticity in the adult visual cortex. *Science* 320(5874):385–388.
50. Baroncelli L, Maffei L, Sale A (2011) New perspectives in amblyopia therapy on adults: A critical role for the excitatory/inhibitory balance. *Front Cell Neurosci* 5:25.
51. Klausberger T, Roberts JDB, Somogyi P (2002) Cell type- and input-specific differences in the number and subtypes of synaptic GABA(A) receptors in the hippocampus. *J Neurosci* 22(7):2513–2521.
52. Schlüter OM, Xu W, Malenka RC (2006) Alternative N-terminal domains of PSD-95 and SAP97 govern activity-dependent regulation of synaptic AMPA receptor function. *Neuron* 51(1):99–111.
53. Elias GM, et al. (2006) Synapse-specific and developmentally regulated targeting of AMPA receptors by a family of MAGUK scaffolding proteins. *Neuron* 52(2):307–320.
54. Freund TF, Katona I (2007) Perisomatic inhibition. *Neuron* 56(1):33–42.
55. Akgul G, Wollmuth LP (2010) Expression pattern of membrane-associated guanylate kinases in interneurons of the visual cortex. *J Comp Neurol* 518(24):4842–4854.
56. Bonnet SAD, et al. (2013) Synaptic state-dependent functional interplay between postsynaptic density-95 and synapse-associated protein 102. *J Neurosci* 33(33): 13398–13409.
57. Restani L, et al. (2009) Functional masking of deprived eye responses by callosal input during ocular dominance plasticity. *Neuron* 64(5):707–718.
58. Migaud M, et al. (1998) Enhanced long-term potentiation and impaired learning in mice with mutant postsynaptic density-95 protein. *Nature* 396(6710):433–439.
59. Rumpel S, Kattenstroth G, Gottmann K (2004) Silent synapses in the immature visual cortex: Layer-specific developmental regulation. *J Neurophysiol* 91(2):1097–1101.
60. Cynader M (1983) Prolonged sensitivity to monocular deprivation in dark-reared cats: Effects of age and visual exposure. *Brain Res* 284(2-3):155–164.
61. Guo Y, et al. (2012) Dark exposure extends the integration window for spike-timing-dependent plasticity. *J Neurosci* 32(43):15027–15035.
62. He H-Y, Hodos W, Quinlan EM (2006) Visual deprivation reactivates rapid ocular dominance plasticity in adult visual cortex. *J Neurosci* 26(11):2951–2955.
63. Morales B, Choi S-Y, Kirkwood A (2002) Dark rearing alters the development of GABAergic transmission in visual cortex. *J Neurosci* 22(18):8084–8090.
64. Philpot BD, Espinosa JS, Bear MF (2003) Evidence for altered NMDA receptor function as a basis for metaplasticity in visual cortex. *J Neurosci* 23(13):5583–5588.
65. Carmignoto G, Vicini S (1992) Activity-dependent decrease in NMDA receptor responses during development of the visual cortex. *Science* 258(5084):1007–1011.
66. Riebe I, Gustafsson B, Hanse E (2009) Silent synapses onto interneurons in the rat CA1 stratum radiatum. *Eur J Neurosci* 29(9):1870–1882.
67. Fagiolini M, Hensch TK (2000) Inhibitory threshold for critical-period activation in primary visual cortex. *Nature* 404(6774):183–186.
68. Chevaleyre V, Castillo PE (2004) Endocannabinoid-mediated metaplasticity in the hippocampus. *Neuron* 43(6):871–881.
69. Greifzu F, et al. (2014) Environmental enrichment extends ocular dominance plasticity into adulthood and protects from stroke-induced impairments of plasticity. *Proc Natl Acad Sci USA* 111(3):1150–1155.
70. Abbas AI, et al. (2009) PSD-95 is essential for hallucinogen and atypical antipsychotic drug actions at serotonin receptors. *J Neurosci* 29(22):7124–7136.
71. Hippenmeyer S, et al. (2005) A developmental switch in the response of DRG neurons to ETS transcription factor signaling. *PLoS Biol* 3(5):e159.
72. Madisen L, et al. (2010) A robust and high-throughput Cre reporting and characterization system for the whole mouse brain. *Nat Neurosci* 13(1):133–140.
73. Cang J, Kalatsky VA, Löwel S, Stryker MP (2005) Optical imaging of the intrinsic signal as a measure of cortical plasticity in the mouse. *Vis Neurosci* 22(5):685–691.
74. Kalatsky VA, Stryker MP (2003) New paradigm for optical imaging: Temporally encoded maps of intrinsic signal. *Neuron* 38(4):529–545.